

# WORLD CEMENT®

March 2015



**HEKO®**  
**Ketten GmbH**





# BOLDROCCHI

ESTABLISHED IN 1909

**Designing and Manufacturing Custom-engineered  
Heavy duty Fans, Dampers and Air Pollution Control  
Systems for any Cement Application**



**Subsidiaries in:**

Germany • France • Egypt • U.S.A. • Mexico • Brasil • India • China

**Group Headquarter:**

Biassono (MI) • Italy • Phone +39 039 2202.1 • Fax +39 039 2754.200 • [boldrocchi@boldrocchi.eu](mailto:boldrocchi@boldrocchi.eu)

**[www.boldrocchi.eu](http://www.boldrocchi.eu)**

Matteo Giavazzi, Boldrocchi s.r.l., Italy, presents a study on dual phase CFD for the dimensioning of flue gas treatment equipment.

# A MODEL SOLUTION

## Abstract

Computational fluid dynamics (CFD) is a computer-aided engineering tool widely used in the dimensioning of industrial equipment. It is used to investigate the thermo and fluid dynamics of flue gas entering the bag filter, ESP and gas conditioning tower.

Real performances of dedusting equipment are sometimes quite different to the ones foreseen during the design phase; gas behaviour inside the equipment is often responsible for the lack of performance.

CFD can calculate the combined effects of fluid flow, heat transfer, mass transfer and species mixing, predicting the real performance. It deals with the complexity of the Navier-Stokes equations, which

describe the flow-related characteristics with a system of non-linear partial differential equations.

This article looks at the analysis of the governing equations at the basis of CFD calculations; the author describes the cases in which a monophasic approach is the optimal solution, as it combines low computational time with good calculations of speed fields; finally, the cases in which a multi-phase approach is required are analysed in order to get a complete investigation of the phenomena occurring inside equipment.

## Methodology definition

The sensibility towards fluid dynamic aspects comes from a long experience with physical filter models.



Lab scale prototypes are usually built scaled 1:8 and respect the law of similitude (ratio between Reynolds number near 1).

Before CFD software, these physical models were used for years to evaluate the effects of deflectors and plates on gas velocity distribution. Moreover, when CFD software was introduced, physical models were used to validate the results obtained from numerical simulations in order to test the accuracy of the tools.

Empirical testing and measurements on physical models also enabled the definition of the most critical aspects in filter design and the best solutions to optimise gas distribution.

Physical models increased the awareness of fluid dynamic problems and encouraged the approach to computational software with higher capabilities for finding easier and effective solutions.

In CFD procedures, the Navier-Stokes equations, which describe the flow-related characteristics with a system of non-linear partial differential equations, are broken down into simpler algebraic expressions, and then integrated over individual computational mesh cells.

The breakdown results in a sub-system of non-linear algebraic equations, which are then solved on a computer.

### Turbulence model

In order to model the turbulent flow, the common Reynolds averaged Navier-Stokes (RANS) approach is used.

A standard 2-equation k-epsilon High Reynolds Number numerical model with logarithmic wall function is applied here.

This kind of turbulence model is based on the eddy viscosity hypothesis, where Reynolds stresses are represented by the effect of additional turbulent viscosity.<sup>1</sup>

### Multi-phase method

The methodology used here is a dispersed multi-phase Eulerian – Lagrangian flow model, where the conservation equations of momentum, heat and mass for the dispersed phase are written for each individual particle.<sup>2</sup>

The dispersed phase is influenced by the continuous phase, and vice versa through interphase momentum, heat and mass transfer.

More precisely, momentum, heat and mass transfer from the dispersed phase leads to a source of momentum, heat and mass in the continuous phase, and vice-versa; then the phases calculation is fully-coupled.

The turbulence effect of fluid velocity on particle motion is accounted for by means of the well-established stochastic technique of Gosman and Ioannides,<sup>2</sup> which introduces the fluctuating nature of the turbulent velocity field, leading to a random turbulent dispersion model of particles.

## Governing equations

### Momentum interphase transfer<sup>3</sup>

The governing equation that describes the interphase momentum transfer between the gaseous phase and the dispersed phase is as follows:

$$m_p \frac{du_p}{dt} = F_{TOT}$$

Where  $F_{TOT}$  is the vector sum of all forces acting on the particles.

In the plants here described, the most important forces acting on the dispersed phase are the drag force and the gravitational buoyancy force.

The drag force equation is:

$$F_{DRAG} = \frac{\rho}{2} C_D A_{pc} |u - u_p| (u - u_p)$$

where  $C_D$  is the drag coefficient and it is defined below:

$$C_D = \begin{cases} \frac{24}{Re_p} & (1 + 0.15 Re_p^{0.687}) \text{ if } Re_p \leq 1000 \\ 0.44 & \text{if } Re_p > 1000 \end{cases}$$

$A_{pc}$  is the particle cross-sectional area, and  $Re_p$  is the Reynolds particle number, defined as:

$$Re_p = \frac{\rho}{\mu} |u - u_p| D_p$$

The gravitational buoyancy force equation is:

$$F_b = \frac{1}{6} \pi D_p^3 \cdot (\rho_p - \rho) \cdot g$$

where  $\rho_p$  is the dispersed phase density, and  $g$  is the gravitational acceleration.

### Heat and mass interphase transfer<sup>4</sup>

The following equation describes the heat conservation and transfer between the gaseous phase and the dispersed phase:

$$\frac{d(m_p C_p T_p)}{dt} = -A_{ps} q_s + h_v \frac{dm_p}{dt}$$

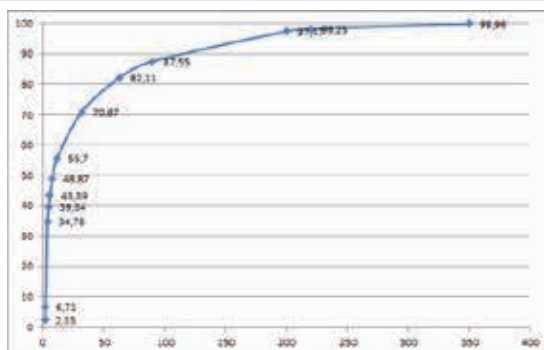
These equations take into account the convection heat transfer and the effects of evaporation latent heat on the particles' internal energy.

The expression used to describe the interphase mass transfer between the continuous phase and the dispersed phase is:

$$\left| \frac{dm_p}{dt} \right| = D_p \cdot (\rho \cdot Diff) \cdot Sh \cdot f(c)$$

**Table 1. Dust diameters distribution**

Dust diameter [µm]	Cumulative mass %
2.00	2.33%
2.50	6.71%
4.00	34.78%
5.00	39.64%
6.00	43.39%
8.00	48.87%
12.00	55.70%
32.00	70.87%
63.00	82.11%
90.00	87.55%
200.00	97.47%
220.00	98.25%
350.00	99.96%
>350	100.00%



Where  $D_p$  is the droplet diameter,  $(\rho \bullet Diff)$  is the dynamic diffusivity of the component in the continuum,  $f(c)$  is a function of migrating component concentrations in both phases, and  $Sh$  is the Sherwood number, given by the following expression:

$$Sh = 2 + 0.6Re_p^{1/2} \left( \frac{\mu}{\rho Diff} \right)^{1/3}$$

$Re_p$  is, as usual, the Reynolds particle number.

If particle temperature exceeds the boiling point, the mass transfer rate is determined by the convective heat flux and the latent heat of vaporisation.

**Table 2. Bag filter process conditions**

Inlet raw gas flow	~400 000 Nm <sup>3</sup> /h
Inlet raw gas temperature	100°C
Filter underpressure	~8000 Pascal at inlet flange
Dust mass flow	~340 000 kg/h

**Table 3. Bag filter dust pre-separation performance**

	Standard filter (reference)	Standard Boldrocchi HD filter	Specific Boldrocchi HD filter
Dust pre-separated in bottom discharge, never reaching bags	>10%	>30%	>35%
Dust reaching bags	<90%	<70%	<65%

### A different approach for each different problem

In CFD analyses, a mono-phase method has advantages and disadvantages over a multi-phase method. Users should carefully check these before deciding which method to use.

Mono-phase is easier to converge than multi-phase, and it requires less

computational time and computer resources, and less custom modelling effort. It is extremely useful when it is necessary to optimise, for example, gas distribution inside a bag filter, in order to feed each bag with equal gas quantity and control can velocity, avoiding dangerous velocity peaks.<sup>5</sup>

However, mono-phase techniques are based on assumptions that, in some particular cases, are not valid and therefore can lead to inaccurate results.

This occurs in 'high dust' bag filters, in 2-fan-systems, where all the raw mill dust reaches the bag filter. This also applies to gas conditioning towers, where it is often useful to simulate the evaporation drop and the interaction between gas and water, besides analysing gas distribution at injection lances level.

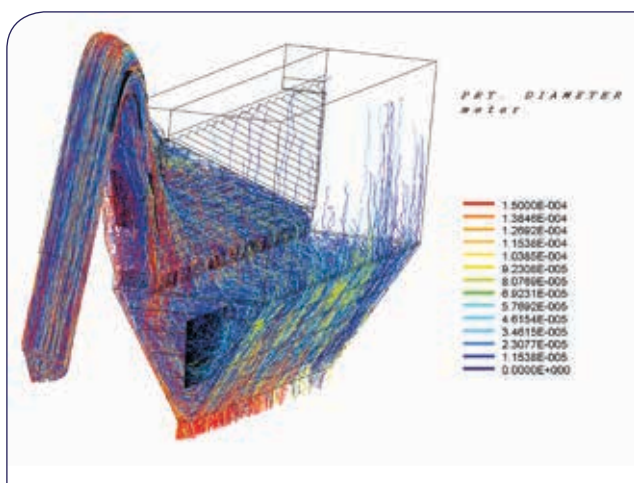


**Figure 1. Particle trajectories and diameters.**

### High dust bag filters

This approach has recently been used to study both the design of new high dust bag filters, and to define a better approach for revamping existing high dust bag filters and for the conversion of ESPs into bag filters.

In all cases, it is critical to use a correct dust diameter distribution input size. Table 1 illustrates a typical cumulative mass percentage as a function of dust diameter.

In the following example a bag filter receives gas and dust from a raw mill with the characteristics of Table 2.

The aim of bag filter design, besides the containment of particulate emission, is the minimisation of pressure drop and maximisation of bag life; these two objectives can be targeted by means of an optimised fluid dynamic behaviour and gas distribution, and a great pre-separation of dust. Catching most particulate matter in the hopper before it reaches the bag's pattern is the key.

Table 3 compares the dust pre-separation obtained in three configurations: a standard bag filter, a Boldrocchi standard design high dust bag filter and a final optimised Boldrocchi design high dust bag filter after dual phase CFD analysis for specified process conditions.

In terms of dust mass, in a standard bag filter, about 272 000 kg/hr (on a total of 340 000) should reach the bags, while in the optimised high dust Boldrocchi bag filter a large percentage of this is pre-separated and avoids increasing bag differential pressure.

Figure 1 shows details of particle trajectories and diameters.

The behaviour of dust particles to be transported by gas or to fall in the hopper as a function of diameter is self-explanatory.

The same technique has been applied in the revamping of the existing high dust bag filter (about 200 000 Nm<sup>3</sup>/h, 850 g/Nm<sup>3</sup>), in which pre-separation performances were not sufficient and the dust feed to bags was not uniformly distributed, thus leading to an unacceptable bag filter pressure drop. In this case, the analysis suggested specific interventions in the hopper area, as shown in Figure 2, which describes dust concentration towards bags before and after modifications (red means 1 kg/Am<sup>3</sup>, green means 0.5 kg/Am<sup>3</sup>).

The different configuration of perforated plates and gas distribution inside hoppers enabled the pre-separation of dust to be increased by 115%. It improved the uniformity of dust distribution reaching the bags and significantly reduced the bag filter pressure drop and the bag cleaning frequency.

Similar results have been obtained in the conversion of high dust ESPs to bag filters.

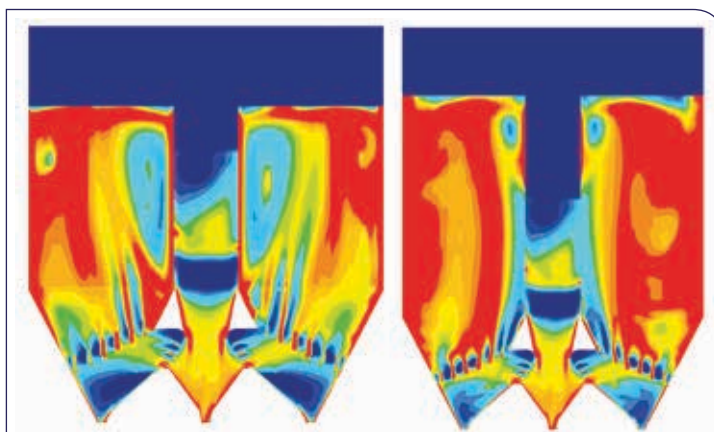


Figure 2. Dust concentration reaching bags from vertical channel.

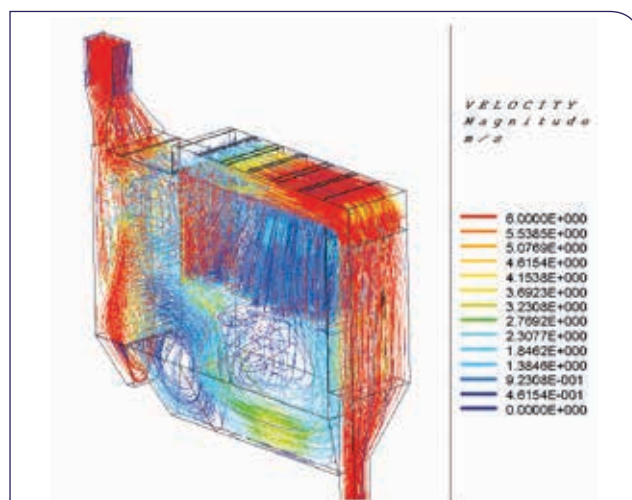


Figure 3. Gas velocity streamlines.

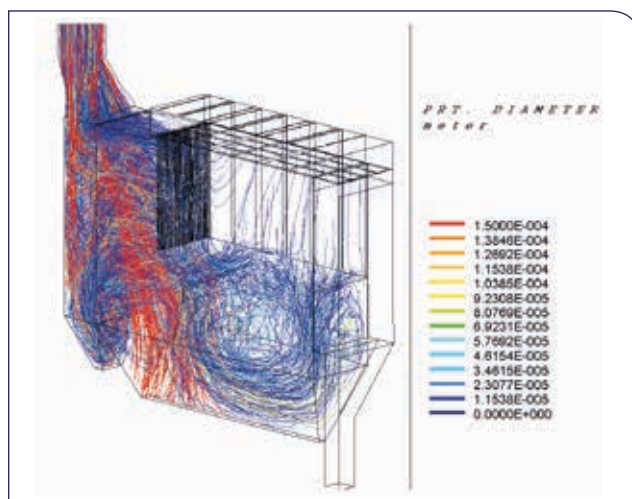


Figure 4. Particle trajectories and diameters.

These kinds of projects typically require a high degree of customisation, as the old ESP casing needs to be adapted to receive bags and all the fluid dynamic behaviour of the equipment has to be modified.

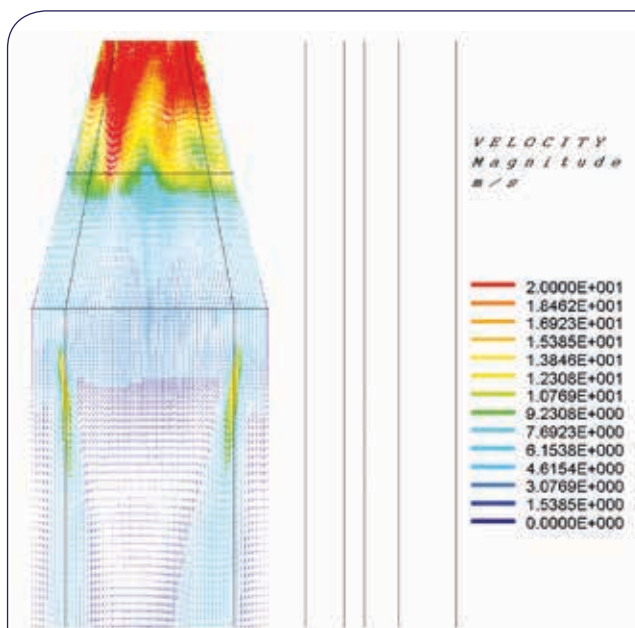


Figure 5. Gas distribution before injection lances.

Table 4. Gas conditioning tower operative conditions

Inlet raw gas flow	~300 000 Nm <sup>3</sup> /h
Inlet raw gas temperature	400°C
Thermal conditions on walls	Adiabatic
Expected outlet temperature	150°C
Sprayed liquid water volume-flow	~50 m <sup>3</sup> /h

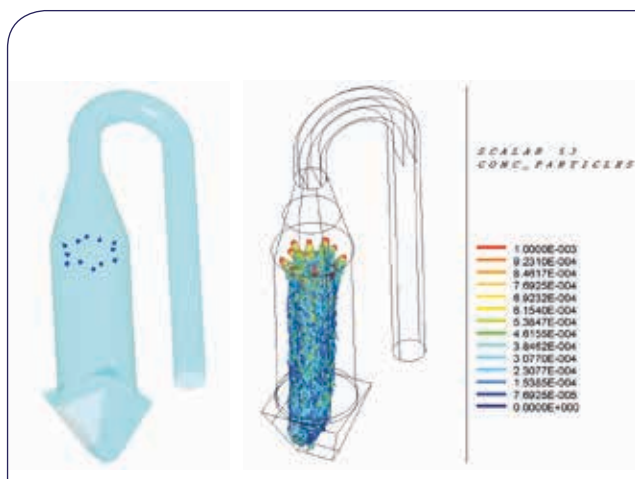


Figure 6. 'Configuration 1' of lance positions.

Table 5. Results: mass-flow of residual liquid water at tower bottom

Analysis	Liquid water mass-flow residual at tower bottom
Configuration 1	7.5547% of injected
Configuration 2	0.0020% of injected

Adding internal deflectors yields the gas distribution pattern of Figure 3. A part of the gas reaches the bags horizontally, and a part with bottom-top direction, ensuring the uniform feeding of the bags.

Figure 4 shows the particles trajectories: those with bigger diameters fall into the first and second hopper, reaching a pre-separation of about 45% (~130 000 kg/hr).

### Gas conditioning towers

Maintaining a homogenous gas distribution is essential in gas conditioning towers. This can be engineered by means of inlet cone and perforated plates. Water is fed into the system (from the top) where gas has a uniform velocity profile, thereby avoiding gas over or underfeeding areas (Figure 5).

Furthermore, it is possible to optimise the position of injection lances in order to optimise drop evaporation.

Starting from drop diameters distribution curves, it is possible to calculate, by means of CFD multi-phase methods, residual dust humidity at tower bottom with different conformations of lance positions and droplet diameter distributions.

In the following example a gas conditioning tower (GCT) installed on a 4200 tpd cement kiln cools the gas with the characteristics shown in Table 4.

It is interesting to compare the performance of the GCT corresponding to different injection lances' geometrical configuration and different drop diameters.

Figures 6 – 9 and Tables 5 – 13 describe the evaporative results, obtained by the standard binary system approach, which is:

1. Gas phase, composed by gas components + dust dispersed component.
2. Liquid phase, composed by liquid water.

There are mainly two degrees of freedom for the position of the lances that can be investigated:

- Lance insertion lengths.
- Angle of spray nozzle.

Figure 6 shows 'Configuration 1' for lance positions and consequent spray cloud water concentration [g/Am<sup>3</sup>].

Figure 7 shows 'Configuration 2' of lance positions and consequent spray cloud water concentration [g/Am<sup>3</sup>].

In other words, changing the injector's position and injection angle has allowed a dramatic reduction in mass flow of residual liquid water at tower bottom, as per Table 5.

Dust moisture is reduced from unacceptable levels (determining mud problems at extraction screw conveyor) to almost dry dust (Table 6).

It is important to underline that the two above configurations are calculated by CFD software in order



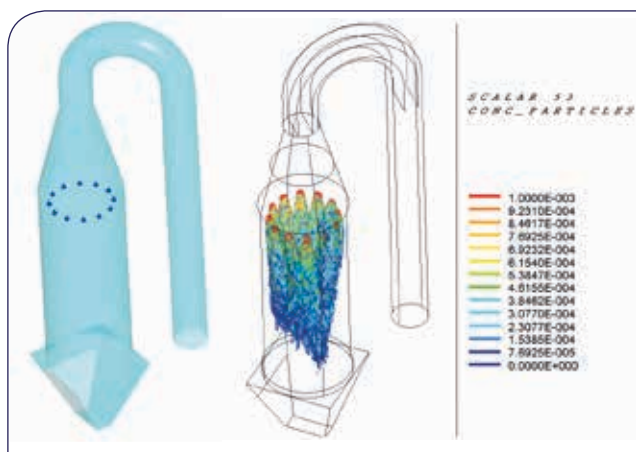


**Figure 7. 'Configuration 2' of lance positions.**

**Table 6. Dust moisture at tower bottom**

Analysis	Dust moisture at tower bottom (wet based percentage)
Configuration 1	25.5 %
Configuration 2	0.2%

**Table 7. Drop size and speed distribution**

	Droplet dia. [ $\mu\text{m}$ ]	Volume %
Average drop dia. (D32 Sauter)	62.9 $\mu\text{m}$	33.5
Maximum drop dia. (Dmax)	155 $\mu\text{m}$	

**Table 8. Drop sizes and speed distribution (worst)**

	Droplet dia. [ $\mu\text{m}$ ]	Volume %
Average drop dia. (D32 Sauter)	101.5 $\mu\text{m}$	33.5
Maximum drop dia. (Dmax)	250 $\mu\text{m}$	

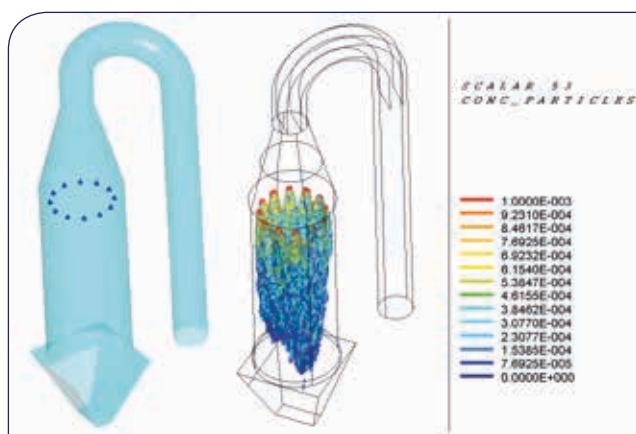


**Figure 8. 'Configuration 3': different droplets size distribution.**

to obtain the same temperature reduction, dosing the same water quantity, starting from the same droplets distribution (Table 7); the only difference influencing the formation of mud at tower bottom is the geometrical configuration of the injection lances.

It is clear how useful it is to be able to test different lance positions and angles and optimise them with a software tool, eliminating any uncertainty and predicting the real performance of the gas conditioning tower in terms of complete evaporation capabilities.

The tool is also useful in order to compare different nozzle performances, selecting the best choice for each individual project.

Table 8 shows a different droplet distribution used to calculate the dust moisture at tower bottom with the same boundary and geometric conditions of 'Configuration 2'.

It is interesting to note how increasing the D32 diameter from 62 to 101  $\mu\text{m}$  increases the dust moisture at tower bottom by five times (Figure 8 and Tables 9 and 10).

Of course, the larger the droplet mean and maximum diameter, the longer the required evaporation time. Gravity force has a greater effect on large drop because they quickly reach the tower bottom, giving rise to wall contact risk.

Other interesting tests can be performed simulating a reduction of droplet velocity injected into the tower. This modification can be harmful: it can produce an insufficient gas-to-liquid relative velocity, with a reduction of evaporation rate in the first stages of the tower; the gas-phase flow can easily bend droplet direction, spreading them against side walls by mean of turbulent interactions.

This effect is evident in Figure 9 (where droplet velocity has been halved in respect to configuration 2). Numerical results are given in Tables 11 and 12.

It is useful to underline the different effect of increasing droplet diameter or the decreasing droplet speed: in both cases the dust moisture at tower bottom increases, but in the first case (diameter) the worst consequence is on the bottom wall, in the second case (speed) it is on the side wall (Table 13).

## Conclusion

In order to decide if one should use a mono or multi-phase CFD approach, it is useful to distinguish the objective of the analysis and the kind of application under examination.

Inside bag filters, heavy particles (dust phase) dispersed in light continuous phase (gas phase), interact with one another exchanging momentum, while interphase heat and mass transfer are generally negligible. Heavy particles will try to deviate from the gas flow path because of gravitational effects (settling) and inertial effects (when flow encounters strong curvatures).



**Table 9. Mass-flow of residual liquid water at tower bottom**

Analysis	Liquid water mass flow residual at tower bottom
Configuration 2	0.0020% of injected
Configuration 3	0.0501% of injected

**Table 10. Dust moisture at tower bottom**

Analysis	Dust moisture at tower bottom (wet-based percentage)
Configuration 2	0.2%
Configuration 3	1.0%

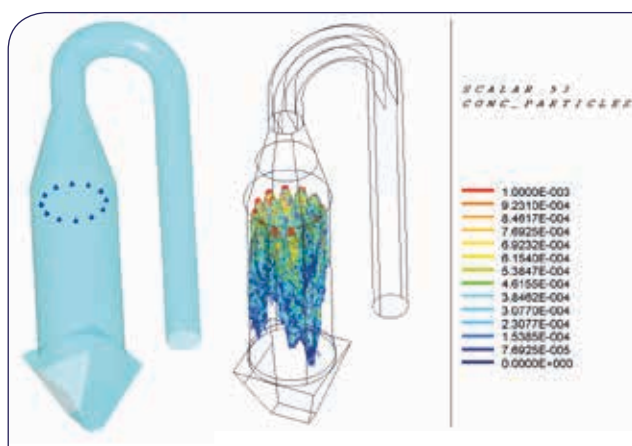


**Figure 9. 'Configuration 4': different droplet velocity.**

**Table 11. Mass-flow of residual liquid water at tower bottom**

Analysis	Liquid water mass-flow residual at tower bottom
Configuration 2	0.0020% of injected
Configuration 4	0.0077% of injected

**Table 12. Dust moisture at tower bottom**

Analysis	Dust moisture at tower bottom (wet-based percentage)
Configuration 2	0.2%
Configuration 4	0.7%

**Table 13. Liquid water splashed on walls (% of injected)**

Analysis	% Liquid water splashed on bottom wall	% Liquid water splashed on side wall	% Liquid water splashed on all walls
Configuration 2	0.0000%	0.0014%	0.0014%
Configuration 3	0.0029%	0.0139%	0.0168%
Configuration 4	0.0047%	0.1462%	0.1508%

## Case 1

When dust concentration is low, the gas behaviour is almost unaffected by powder and the mono-phase analyses can calculate with good approximation the gas flow characteristics.

## Case 2

When dust load increases, the monophasic approach gradually loses its validity. In these situations, the dispersed phase has enough momentum to bend gas streamlines and it can also affect the continuous phase motion.

In the latter case multi-phase approaches are recommended, not only to analyse the dust phase features, but also to correctly predict the gas-phase flow itself.

In gas conditioning towers physical interactions are far more complex. In fact, in GCTs the coupling between phases is very strong, because particles and gas can exchange momentum, heat, mass and species concentrations at the same time.

Furthermore, in these plants the flow regime is generally compressible, because of the significant latent heat evaporation, which strongly affects temperature, density and therefore the aerodynamic behaviour of the gas phase.

As a result, the effects exerted by the dispersed phase on gas phase are always important, also when particle loading is very low and their momentum effects on continuous phase could be negligible.

Therefore, in this kind of evaporative equipment, CFD analysis is a generally accepted tool used for multi-phase predictions with nearly any dispersed phase concentration range. 🌐

## References

1. LAUNDER, B.E., SPALDING, D.B., 1972. *Mathematical Models of Turbulence*, Academic Press, London.
2. GOSMAN, A.D. and IOANNIDES, E., 1983. 'Aspects of computer simulation of liquid-fueled combustors', *J. Energy* 7, 482 – 490.
3. SCHILLER, L. and NAUMANN, A., 1933. 'Über die grundlegenden Berechnungen bei der Schwerkraftaufbereitung', *Ztg. Ver. Deut. Ing.* 77, 318 – 320.
4. RANZ, W.E. and MARSHALL, W.R., (1952). 'Evaporation from Drops, Part I', *Chemical Engineering Progress*, 48, 141 – 146.
5. COLOMBO, E., INZOLI, F., BONALUMI, D., MIGLIETTA, F. and GIAVAZZI, M., 'Flow dynamic analysis and optimization of an industrial bag filter', *XXVII UIT CONGRESS 2009*.

## Note

All the projects described in this article have been performed with the help of Eng. G. Pesenti, CFD specialist, and M. Stoppa, 3D mechanical design specialist.